Journal of Thermal Analysis and Calorimetry, Vol. 83 (2006) 1, 91–95

FINITE ELEMENT MODELING OF SYNTACTIC FOAM

M. L. Hobbs[*]

Thermal and Reactive Processes, Org. 9116, MS0836, Engineering Sciences Center, Sandia National Laboratories
P.O. Box 5800, Albuquerque, NM 87111, USA[**]

A decomposition model has been developed to predict the response of removable syntactic foam (RSF) exposed to fire-like heat fluxes. RSF consists of glass micro-balloons (GMB) in a cured epoxy polymer matrix. A chemistry model is presented based on the chemical structure of the epoxy polymer, mass transport of polymer fragments to the bulk gas, and vapor-liquid equilibrium. Thermophysical properties were estimated from measurements. A bubble nucleation, growth, and coalescence model was used to describe changes in properties with the extent of reaction. Decomposition of a strand of syntactic foam exposed to high temperatures was simulated.

Keywords: *decomposition, effective thermal conductivity, lattice statistics, mass transport, removable syntactic foam*

Introduction

RSF encapsulants with low thermal expansion coefficients and high dielectric strengths are used to isolate electronic boards within metal enclosures for protection from shock, vibration, moisture, thermal and electrical environments. The enclosures may have openings that provide pathways for decomposition gases to exit the system when exposed to fire environments. Conversely, some enclosures are hermetically sealed to prevent gases from entering or exiting the system. Consequently, a decomposition model was needed with the ability to predict decomposition behavior associated with both confinement and venting of the decomposition gases as well as pressurization. This paper describes a model for foams exposed to fire-like environments.

Loy *et al.*[1–3] recently patented a method to make thermally removable epoxy foam (REF) that can be removed from potted assemblies with a mild solvent (e.g., *n*-butanol) at 90°C by incorporating chemically labile linkages within a cross-linked polymeric network using the reversible (retro) Diels–Alder reaction. The polymeric matrix for both RSF and REF are essentially the same, except that RSF contains 0.004cm GMB and REF contains 0.03cm bubbles created with a perfluorohexane blowing agent.

The RSF decomposition model is based on a previously developed simple removable epoxy foam (SREF) decomposition model [4]. The RSF polymer lattice structure was inferred from the foam synthesis method as discussed by Clayton [5]. A 3-step kinetic mechanism describes the thermal evolution of bridge populations; lattice statistics describes the dynamic distribution of polymer fragments; and vapor-liquid equilibrium describes partitioning of polymer fragments into condensed- and gas-phases. The gas-phase products are assumed to accumulate in spherical defects, which grow and coalesce based on the decomposition chemistry model and conservation of mass.

Chemical structure and simple lattice

Figures 1 and 2 show the most probable repeating unit of the RSF polymer and a model lattice with a single site highlighted. The lattice is essentially an infinite network, composed of various sites and bridges made from ingredients used to synthesize the polymer. Hobbs [4] gives the coordination number of the model lattice as three, ($\sigma+1=3$).

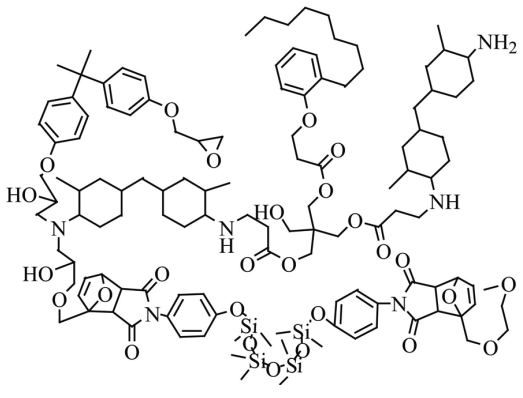

Fig. 1 Most probable unit of RSF polymer

* mlhobbs@sandia.gov

** Sandia is a multiprogram laboratory operated by Sandia Corporation, a Lockheed Martin Company, for the United States Department of Energy's National Nuclear Security Administration under Contract DE-AC04-94AL85000

1388–6150/$20.00

Akadémiai Kiadó, Budapest, Hungary
Springer, Dordrecht, The Netherlands

Mechanism

Figure 3 shows a typical mass loss profile for REF plotted as the normalized sample mass or solid fraction (S_f=m/m_o) for a 5 mg sample heated at 20°C min^{-1} [5]. Figure 3 also shows the rate of mass loss divided by the heating rate ($-dS_f/dT$). The four peaks labeled A–D in Fig. 3 indicate multiple, temperature-dependent reaction steps. Erickson *et al.* [6] have monitored the decomposition gases from thermogravimetric analysis (TG) of REF using real-time FTIR and have periodically analyzed gas samples using a gas chromatograph and mass spectrometer (GC/MS). From room temperature to about 140°C (peak A in Fig. 3), the most abundant decomposition products were the blowing agent and siloxanes associated with the surfactant. From about 140–300°C (peak B in Fig. 3), the major decomposition product was octamethylcyclotetrasiloxane (OS). Peaks C and D are associated with a mixture of products (MP) that include 2-methylfuran, phenol, toluene, nonylphenol (NP), and bisphenol-A (BPA). Less volatile products such as BPA are more prevalent in the fourth peak labeled D in Fig. 3.

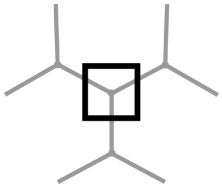

Fig. 2 Model lattice for RSF polymer

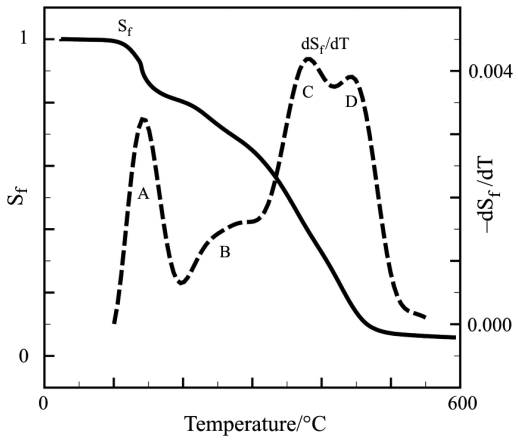

Fig. 3 TG mass loss and rate of mass loss from 4.7–mg REF sample heated at 20°C min^{-1} with A–D showing four primary decomposition steps

Since the RSF does not contain blowing agent or surfactant, only three reactions are needed to describe decomposition products associated with the polymer. These three reactions are used to describe mass loss associated with OS, MP and BPA, and correspond to peaks B–D in Fig. 3. The reactions, mechanism, rate equations, and initial mass fraction based population variables are given in Table 1. Reversible reactions were not included since the model application is for RSF exposed to hydrocarbon fuel fires where reversible reactions are inconsequential.

The mass-based populations; L_1, L_2 and L_3; represent the labile bridges composed of OS, MP and BPA, respectively. OS, MP and BPA are also mass-based population variables, which can be obtained using conservation of mass as follows:

$$\text{OS}=L_1^0-L_1;\ \text{MP}=L_2^0-L_2 \text{ and BPA} = L_3^0-L_3 \quad (1)$$

L_1^0 represents the initial mass fraction of the siloxane moiety in the removable resin that decomposes as OS, L_2^0 represents the initial mass fraction of the polymer that decomposes as MP, and L_3^0 represents the initial mass fraction of the polymer that decomposes as BPA.

The rate constants given in Table 1 are effective rate constants:

$$k_j = 1/[(1/k_j^c+1/k_j^m)] \quad (2)$$

k_j^c and k_j^m represent the kinetic and mass transport rate constants, respectively, k_j^c is:

$$k_j^c=A_j \exp[-(E_j + z_j\sigma_j)/RT] \quad (3)$$

where A represents the pre-exponential factors ($2\cdot10^{15}$, $2\cdot10^{16}$ and $6\cdot10^{12}$, for reactions (1)–(3), respectively [4]. E represents the mean activation energies (53.7, 58.1 and 45.8 kcal mol^{-1} for reactions (1)–(3), respectively) [4]. σ represents the standard deviation parameter used with the distributed activation energy model (4.96, 7.29 and 4.99 kcal mol^{-1} for reactions (1)–(3), respectively, [4]). z, R and T are the ordinate of the cumulative distribution factor (Φ), gas constant, and temperature, respectively. The subscript

Table 1 Mechanism, rate equations and initial conditions for the RSF model

Rxns.	Mechanism	Rate Eqs	M_w/g mol^{-1}	Initial conditions	$D_{j,STP}^m$/cm^2 s^{-1}
1	$L_1 \rightarrow$OS	$r_2=k_2L_1$	$M_{w_{OS}}=296$	L_1^0=0.103	0.0067
2	$L_2 \rightarrow$MP	$r_3=k_3L_2$	$M_{w_{MP}}$=140	L_2^0=0.557	0.0062
3	$L_3 \rightarrow$BPA	$r_4=k_4L_3$	$M_{w_{BPA}}$=228	L_3^0=0.090	0.0213
			$M_{w_{residue}}$=1000	residue=0.25*	

*The residue is the equilibrium value and is not determined with any kinetic mechanism.

j refers to reactions (1)–(3) in Table 1. The reactions are distributed with the extent of bridge breaking as follows:

$$\Phi(z)=1-p=\int_{-\infty}^{z}\frac{1}{\sqrt{2\pi}}\exp(-\frac{1}{2}z^2)\mathrm{d}z \quad (4)$$

where p is the bridge population, $p=(L_1+L_2+L_3)/(1-\text{residue})$.

For unconfined decomposition, the mass transport rate constant in Eq. (4) is

$$k_j^m = S_f / D_j^m \quad (5)$$

The mass diffusivities, D_j^m, all have the following temperature dependency:

$$D_j^m = D_{j,STP}^m (T/298.15)^{1.5} \quad (6)$$

$D_{j,STP}^m$ are the mass diffusivities at standard temperature and pressure given in Table 1.

Lattice statistics

The mass of the RSF site shown in Fig. 2, m_t, depends on the average molecular mass of the bridges connecting the sites, $\overline{M}_b$, 172 g mol^{-1}, as follows:

$$m_t = 3/2\overline{M}_b \quad (7)$$

The factor 3/2 represents three half bridges enclosed with the black square in Fig. 2. A monomer contains a single site, a dimer contains two sites connected by a bridge, and a trimer contains three sites connected by two bridges. In the RSF lattice model, bridges are either occupied or unoccupied, implying that monomers do not have mass. The molecular mass of an *n*-mer, M_n, is $(n-1)\overline{M}_b$.

Mass fractions of OS, MP and BPA (ω_{OS}, ω_{MP} and ω_{BPA}) can be determined from the population variables. Mass fractions of *n*-mers, $\omega_{n\text{-mer}}$, are

$$\omega_{n\text{-mer}} = \frac{2/3(n-1)}{n}\left[\frac{\sigma+1}{\tau+s}\binom{\tau+s}{n-1}p^s(1-p)^\tau\right] \quad (8)$$

as discussed by Hobbs [4]. τ is the number of broken bridges on the perimeter of the polymer fragment with *s*-bridges connecting *n*-sites. The factor $\frac{\sigma+1}{\tau+s}$ converts from a bridge basis to a site basis. The binomial expression, $\binom{\tau+s}{n-1}$, represents the number of distinct *n*-mer configurations that can be obtained from $\tau + s$ potential bridges.

The RSF model considers 7 species – 1) OS, 2) MP, 3) BPA, 4) 2-mers, 5) 3-mers, 6) 4-mers, 7) non-volatile residue. The non-volatile residue mass is obtained by:

$$\omega_{residue}=1-\omega_{OS}-\omega_{MP}-\omega_{BPA}-\omega_{2\text{-mer}}-\omega_{3\text{-mer}}-\omega_{4\text{-mer}} \quad (9)$$

Molecular masses for the OS, MP and BPA were given in Table 1; and molecular masses for the 2-mers, 3-mers, and 4-mers are $(n-1)\overline{M}_b$ where $\overline{M}_b$ is 172 g mol^{-1}.

Vapor-liquid equilibrium

The split between vapor and condensed species was determined using a standard multicomponent flash calculation as discussed in detail by Hobbs [4]. The activity coefficients were chosen to limit the influence of pressure above critical conditions as follows:

$$\gamma_i = \begin{cases} \gamma_i^0 & \text{if } P \le P_{c,i} \\ \gamma_i^0 P/P_{c,i} & \text{if } P > P_{c,i} \end{cases}, \quad (10)$$

where γ_i^0 , P and $P_{c,i}$ represent the activity coefficients of the i^{th} species at ambient conditions, the thermodynamic pressure, and the critical pressure of the i^{th} species, respectively. The effect of the activity coefficient model is to prevent the vapor-liquid equilibrium ratio or *K*-value from approaching zero as pressure exceeds the critical pressure. Hobbs [4] gives $\gamma_i^0=0.5$ for all of the species except for MP, which is $\gamma_{MP}^0=3$. Hobbs [4] also uses 13.1, 52.0, 28.9, 38.7, 38.7 and 38.7 atm for the critical pressures of OS, MP, BPA, 2-mers, 3-mers, and 4-mers. The critical pressures of the mers were assumed to be the average critical pressure of various cresols, phenols, and furans. Hobbs [4] gives the temperature dependent vapor pressures used for various RSF species.

Effective thermal conductivity

One potential mechanism of heat transfer in RSF is based on the effective thermal conductivity of the foam:

$$\lambda_{eff}=\phi\lambda_{decomposition\ gases}+(1-\phi)\lambda_{condensed\text{-}phases}+4\sigma_{sb}T^3a \quad (11)$$

where ϕ is the gas volume fraction, $\lambda_{decomposition\ gases}$ is the gas thermal conductivity, $\lambda_{condensed\text{-}phase}$ is the condensed-phase thermal conductivity, σ_{sb} is the Stefan–Boltzmann constant, and T is temperature. 'a' is the spherical defects diameter determined as follows:

$$a = (6m_g/\pi\rho_g)^{1/3} = \\ = (6[\rho_g^0 V_g^0 + \rho_c^0 V_c^0 (1-S_f)]/\pi\rho_g)^{1/3} \quad (12)$$

where m_g and ρ_g are the mass and density of the gas, respectively. The gas mass is the initial gas mass ($\rho_g^0 V_g^0$) plus the gases produced via decomposition $[\rho_c^0 V_c^0 (1-S_f)]$. The gas volume fraction, ϕ, can be calculated from

$$\phi=(m_g/\rho_g)/[(m_g/\rho_g)+(m_c/\rho_c)] \quad (13)$$

where m_c and ρ_c are the mass and density of the condensed-products, respectively. The condensed-phase mass is a function of the solid fraction, $(\rho_c^0 V_c^0 S_f)$.

Finite element implementation

The response of the RSF encapsulant was determined with a finite element model that solves the heat diffusion equation with a source term for chemistry:

$$\rho C\frac{\partial T}{\partial t}=\frac{\partial}{\partial x}\left(\lambda_{\text{eff}}\frac{\partial T}{\partial x}\right)+\sum_{i=1}^{3} q_i r_i \quad (14)$$

where q_i is the reaction enthalpy which is assumed to be –11, –101 and +82 cal g^{-1} for reactions (1)–(3), respectively. The species equations, $dL_i/dt=r_i$, are solved with Eq. (14), at each integration or Gauss point in the finite element model.

Results

Figure 4 shows the predicted mass loss and rate of mass loss at a single integration point using both the SREF and RSF decomposition models. The primary differences between SREF and RSF results are that the SREF shows early mass loss associated with desorption of the blowing agent. The initial decomposition of the RSF is due to the release of OS. The SREF model predicts a 5% carbonaceous residue. The RSF model predicts the same 5% carbonaceous residue, but also includes an additional 20% residue due to GMB, which is assumed to be nonvolatile.

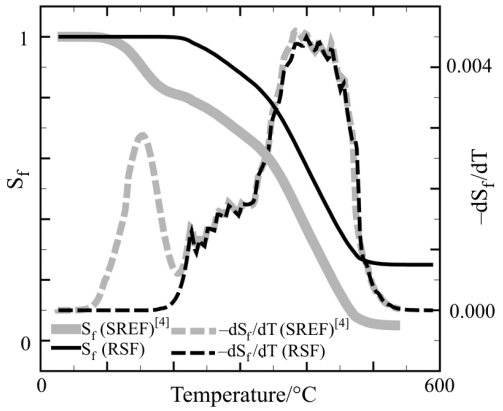

Fig. 4 Mass loss and rate of mass

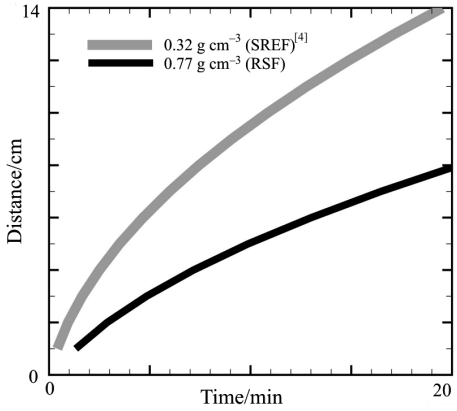

Fig. 5 Predicted front location

Figure 5 shows the predicted locations of the decomposition front in a strand of 0.77 g cm^{-3} RSF and a strand of 0.32 g cm^{-3} REF exposed at one end to 1.000°C temperature with the remaining sides insulated. The initial defect diameter (a fitting parameter) was assumed to be 0.15 cm for both strands. The RSF strand decomposes slower than the SREF strand due to the higher density and slower decomposition rates.

Conclusions

A thermal decomposition model for RSF has been described that uses a three-step mechanism with mass transport to portray irreversible degradation of RSF. Twenty-five mass percent of the RSF was assumed to be non-volatile. A lattice statistics model determined the 2-mer, 3-mer, and 4-mer populations. Vapor-liquid equilibrium with pressure dependent activity coefficients determined the split between vapor and liquid-phases. Decomposition products accumulating in spherical defects were used to describe the thermal conductivity of the foam. The model was implemented into a finite element code and location of the decomposition front in a strand of foam exposed to a radiation boundary temperature was determined. RSF results were compared to a model of REF that included blowing agent in lieu of GMB. Mass loss was delayed for RSF when compared to REF since no blowing agent was adsorbed onto the polymer matrix. Slower decomposition rates for RSF were also attributed to higher density.

Acknowledgements

I thank the numerous people at Sandia National Laboratories and Brigham Young University that have provided much assistance. Tom Fletcher and Dan Clayton supplied the mass loss data in Fig. 3. Bill Erikson and Amy Sun provided insightful comments regarding the manuscript.

References

1 Patent #6,337,384, Method of Making Thermally Removable Epoxies, 2002.

2 J. H. Aubert, J. R. McElhanon, R. S. Saunders, P. S. Sawyer, D. R. Wheeler, E. M. Russick, P. B. Rand and D. A. Loy, Progress in Developing Removable Foams, Adhesives, and Conformal Coatings for the Encapsulation of Weapon Components, Sandia National Laboratories Report SAND2001-0295, Albuquerque, New Mexico 2001.

3 J. R. McElhanon, E. M. Russick, D. R. Wheeler, D. A. Loy and J. H. Aubert, J. Appl. Polym. Sci., 85 (2002) 1496.

4 M. L. Hobbs, Polymer Degradation and Stability, 89 (2005) 353.

5 D. J. Clayton, Modeling Flow Effects During Polymer Decomposition using Percolation Lattice Statistics, Dissertation, Brigham Young University, Provo UT 2002.

6 K. L. Erickson, S. M. Trujillo, K. R. Thompson, A. C. Sun, M. L. Hobbs and K. J. Dowding, in A. A. Mammolil and C. A. Brebbia (Eds), Computational Methods in Materials Characterisation, Southampton: WIT Press, (2004) p. 217.

DOI: 10.1007/s10973-005-7098-5